Molecular Catalysis 538 (2023) 112992

Contents lists available at ScienceDirect

Molecular Catalysis

journal homepage: www.journals.elsevier.com/molecular-catalysis

Influence of structural properties of zinc complexes with N4-donor ligands on the catalyzed cycloaddition of CO_2 to epoxides into cyclic carbonates

Nassima El Aouni [a,b], Claudia López Redondo [a], Md Bin Yeamin [a], Ali Aghmiz [b], Mar Reguero [a,*], Anna M. Masdeu-Bultó [a,*]

[a] Department of Physical and Inorganic Chemistry, Universitat Rovira i Virgili, Carrer Marcel·lí Domingo, 1. Campus Sescelades, Tarragona 43007, Spain
[b] Equipe d'Écotoxicologie Marine, FS, Abdelmalek Essaadi University, Tétouan, Morocco

ARTICLE INFO

Keywords:
Cyclic carbonates
Zinc complexes
N4-donor ligands
Schiff base ligands
Carbon dioxide
DFT calculations

ABSTRACT

Zinc(II) complexes [Zn(**L1**-**L5**)Cl_2] with tetra-aza donor ligands bearing phenanthroline and bipyridine bis(aniline) skeleton **L1**-**L5** have been prepared and characterised. These ligands were selected to analyse the influence on the catalytic activity for the CO_2-cycloaddition to epoxides of three parameters: the steric hindrance of the *orto* substituent of the aniline ring, the central skeleton and the nature of the non-aromatic amine. X-ray diffraction characterisation of [Zn(**L1**)Cl_2] and [Zn(**L2**)Cl_2] showed that the geometry is pentacoordinate while in the case of [Zn(**L5**)Cl_2] a four-coordinate tetrahedral complex was formed. Computational calculations using density functional theory methods (DFT) agreed with these results. These complexes combined with tetrabutylammonium bromide (TBAB) are very selective for the CO_2/terminal epoxides coupling to form cyclic carbonates providing activity up to TOF 565 h^{-1}.

1. Introduction

Cyclic organic carbonates such as ethylene and propylene carbonate have industrial interest due to their applications *e.g.* as polar aprotic solvents [1–3], electrolytes in lithium-ion batteries [4], industrial lubricants [5], monomers for polymer synthesis [6–8], or as useful intermediates for the preparation of a wide variety of organic chemical products [9,10]. The most important method to prepare organic carbonates is the phosgenation of alcohols, which involves a highly toxic substance such as carbonyl dichloride [11]. Other possible routes such as the oxidative carbonylation of alcohols use potential explosive carbon monoxide and oxygen mixtures [11]. The greenest, cheapest and most atom-economy efficient synthesis of carbonates is the catalysed cycloaddition of carbon dioxide to epoxides (Scheme 1) [12]. Catalysts for this transformation include organocatalysts such as organic salts [13–16], ionic liquids [17–20] and hydrogen bond donor compounds [21–25]. Metal-based catalytic systems are also used such as metal halides [26,27], metal oxides [28], metal complexes [29–34], or metal-organic frameworks [35,36].

The generally accepted mechanism for this reaction involves, in most cases, three steps starting with the ring opening of the epoxide followed by the insertion of carbon dioxide and finally the ring-closing step to form the cyclic carbonate (Scheme 2) [12,37–43]. The first step is initiated by a nucleophilic attack of a Lewis base (Nu^-, Scheme 2a) to open the epoxide ring. It often corresponds with the highest energetic barrier that is decreased by activating the epoxide with a Lewis acid (LA) or a hydrogen-bond donor (HBD). Next, the alkoxide formed attacks the electrophilic carbon of CO_2 to form a carboxylate species (Scheme 2b). Finally, the nucleophilic attack of the carboxylate on the chain carbon leads to the cyclic carbonate while the nucleophile is released (Scheme 2c). Alternatively, in the last step, the insertion of an epoxide molecule can occur to initiate a copolymerization sequence to form polycarbonates. The relative stability of these intermediates is crucial to selectively form the cyclic carbonates.

Zinc (II)-based complexes are one of the preferred families of catalysts for this reaction for different reasons. One is that they mimic the active site of some biological systems like the carbonic anhydrases, which are involved in the transformation of CO_2 into organic carbonates [44]. Also, zinc is an abundant first-row transition metal with low toxic compounds and it efficiently activates epoxides as a Lewis acid [45]. Zn (II) complexes with Schiff base ligands with N4-donor atoms have been used as catalysts for CO_2/epoxide cycloaddition [46–51] because they are easy to prepare and thus, by modification of the structure, their stereoelectronic properties can be readily modulated. Furthermore,

* Corresponding authors.
E-mail addresses: mar.reguero@urv.cat (M. Reguero), annamaria.masdeu@urv.cat (A.M. Masdeu-Bultó).

https://doi.org/10.1016/j.mcat.2023.112992
Received 23 November 2022; Received in revised form 26 January 2023; Accepted 31 January 2023
Available online 11 February 2023

these complexes may adopt different coordination numbers from 4 to 6, thus, they can stabilize a wide range of geometries [52,53]. This feature may lead to stabilise the catalytic intermediates and modifying their catalytic activity and selectivity. But to improve their performance, detailed knowledge of their structure and their catalytic mechanism must be acquired. In fact, the capacity of N4-ligands to adopt either tri- or tetra-dentate binding modes on coordination to a Zn(II) metallic centre can be assessed from density functional theory (DFT) computational calculations by comparison of the relative energies of these coordination conformers [54] and mechanistic studies can also be developed with similar computational tools.

Regarding the application of Zn-N4-donor ligands as catalysts for CO_2/epoxide cycloaddition, some significant examples have been reported in the literature. The authors of these works use rather high loadings of catalysts or harsh reaction conditions. For instance, Zn halide complexes derived from the N4-donor polypodal ligand tren (N^1,N^1-bis(2-aminoethyl)ethane-1,2-diamine) with formula [Zn(trenR)X]X (X=Br, I) produced cyclic carbonates from terminal epoxides in 80–97% yield at 80 °C under atmospheric CO_2 pressure using 1 mol% catalyst in 6 h [55]. Other Zn-N4-donor catalysts with a pyridine based macrocyclic ligand 3,6,9-triaza-1(2,6)-pyridinecyclodecaphane gave quantitative yields in the cyclic carbonates using 0.5 mol% of catalyst loading at 8 bar of CO_2 pressure at 125 °C at 3 h reaction time [56]. Dinuclear Zn(II) systems with N4-donor and N5-donor ligands based on pyrrole skeleton were also reported to catalyse the cycloaddition of CO_2 to epoxides with TOF up to 232 h^{-1} at 120 °C for styrene oxide in the presence of ammonium halides [57].

Therefore, further developments in this area are still necessary to find more active systems under mild reaction conditions.

In this paper, we report the synthesis and characterization of a series of Zn(II) complexes with 2,9-phenanthroline and 2,2′-bipyridine bis (imine) and bis(amine) ligands N4-donor (**L1**-**L5**, Scheme 3), their application as catalysts for the cycloaddition of carbon dioxide to epoxides to form cyclic carbonates, and the analysis of how different characteristics of the catalysts affect their performance. The effect of the aromatic framework was analysed employing phenanthroline (**L1**-**L3**, Scheme 3) and bipyridine (**L4**-**L5**, Scheme 3) derived ligands. To assess the effect of the steric hindrance around the aniline substituent, different *orto*-substituted anilines were used (**L1**-**L3**, Scheme 3). Finally, the nature of the terminal groups was analysed by reducing the imine groups to amine groups (**L5**, Scheme 3). The information collected with this study will be essential, once the mechanism of the reaction is known, to propose modifications on the catalytic systems to improve their performance.

2. Experimental section

1,10-phenanthroline-2,9-dicarbaldehide [58], 1,1′-(1,10-phenanthroline-2,9-diyl)bis(N-(2,6-diisopropylphenyl)methanimine) (**L1**) [59] and 1,1′-(1,10-phenanthroline-2,9-diyl)bis(N-(3,4-dimethoxyphenyl) methanimine) (**L3**) [60], 2,2′-bipyridine-6,6′-dicarbaldehyde [61,62] and 1,1′-([2,2′-*bi-pyridine*]−6,6′-diyl)bis(N-(2,6-diisopropylphenyl) methanimine) [63] (**L4**) were prepared as described elsewhere. 1,1′-(1, 10-phenanthroline-2,9-diyl)bis(N-(2,6-diethylphenyl)-methanimine (**L2**) was prepared by a similar procedure (See Supplementary Information) [59]. The synthesis of N,N'-(2,2′-bi-pyridine-6,6′-diylbis (methylene))bis(2,6-diisopropylaniline)) (**L5**) is described in Supplementary Information. Ethanol, propanol and butanol were dried with Mg/I_2 under reflux and distilled under nitrogen. Reagents were purchased at Sigma-Aldrich and used as received. Solvents were purified by the system Braun MB SPS-800 and stored under nitrogen atmosphere. Carbon dioxide (SCF Grade, 99.999%, Air Products) was used introducing an oxygen/moisture trap in the line (Agilent). FT-IR (Fourier Transformed Infrared) spectra were recorded on a Brucker Vortex 70 spectrometer and an FTIR JASCO 6700 equipment using the attenuated total reflectance (ATR) technique (range 4000–600 cm^{-1}). Nuclear magnetic resonance NMR spectra were recorded at 400 MHz Varian, with tetramethylsilane (^{1}H NMR and ^{13}C NMR) as internal standards. High resolution electrospray ionization mass spectra (ESI-MS) and elemental analyses were performed at the *Serveis Tècnics de Recerca* from the *Universitat de Girona* (Spain).

2.1. Synthesis of complexes

2.1.1. Synthesis of dichloro(1,1′-(1,10-phenanthroline-2,9-diyl)bis(N-(2,6-diisopropylphenyl)-methanimine))zinc(II) (Zn1)

In a purged Schlenk tube under nitrogen, a mixture of $ZnCl_2$ (0.07 g, 0.51 mmol) and dry propanol (17 mL) was refluxed under stirring until the dissolution of the zinc salt. Then, **L1** was added (0.13 g, 0.23 mmol). A yellow solid precipitated and the mixture was stirred under reflux for 18 h. After cooling to room temperature, the solid was filtered off, washed with dry hexane and dried in vacuum to afford a yellow solid. 0.1100 g. Yield: 64%.

One-pot synthesis of **Zn1**. In a three-neck round bottom flask equipped with a condenser and under nitrogen, 1,10-phenanthroline-2,9-dicarbaldehyde (0.0488 g, 0.23 mmol) was dissolved in dry propanol (10 mL). The solution was heated up to reflux until the dialdehyde was dissolved, then a solution of anhydrous $ZnCl_2$ (0.070 g, 0.51 mmol) in 10 mL of dry propanol was added. Next, a solution of 2,5-diisopropylamine (700 μL, 3.70 mmol) in 10 mL of dry propanol was added dropwise for 30 min. A yellow precipitate appeared. The mixture was stirred under reflux for 18 h. After that time, it was cooled down and the yellow solid was separated by filtration, washed with dry hexane, and dried under vacuum. 0.0724 g. Yield: 46%.

Crystals of **Zn1** suitable for X-ray diffraction analysis were obtained by slow diffusion of hexane into a solution of the complex in deuterated chloroform forming two layers standing in an NMR tube at −30 °C for one week.

Anal. Calcd. For $C_{38}H_{42}Cl_2N_4Zn{\cdot}H_2O$ (709.1): C 64.4, H 6.2, N 7.9; found C 64.2, H 6.0, N 7.7. HRMS (ESI-TOF) *m/z* Calcd. For $C_{38}H_{42}ClN_4Zn$: 653.2389 $[M\text{-}Cl]^+$, found: 653.2379 (100%). ^{1}H NMR (400 MHz, ppm, CD_2Cl_2) δ: 1.18 (d, 24 H, CH_3, J = 6.8 Hz), 3.19 (stp, 4H, CH iPr, J = 6.8 Hz), 7.18–7.24 (m, 6H, CH Ar), 8.19 (s, 2H, CH phen), 8.63 (d, 2H, CH phen, J = 8.4 Hz), 8.78 (d, 2H, CH phen, J = 8.4 Hz), 8.99 (s, 2H, CH═N). ^{13}C NMR (126 MHz, ppm, CD_2Cl_2) δ: 23.8, 27.9, 123.3, 124.9, 125.7, 128.0, 130.8, 138.0, 140.4, 160.0. FTIR (cm^{-1},ATR): 2961 (s), 2921 (w), 2862 (w), 1639 (m, C = N) 1620 (m, C = N), 1587 (m), 1566 (w), 1506 (s), 1462 (s). Conductivity: 0.23 S·cm^2/mol a T = 23.5 °C (CH_2Cl_2, 0.4 10^{-3} M).

2.1.2. Synthesis of dichloro(1,1′-(1,10-phenanthroline-2,9-diyl)bis(N-(2,6-diethylphenyl)-methanimine))zinc(II) (Zn2)

In a purged Schlenk tube under nitrogen, a mixture of $ZnCl_2$ (0.07 g, 0.51 mmol) and dry propanol (17 mL) was refluxed under stirring until the dissolution of the zinc salt. Then, **L2** was added (0.12 g, 0.23 mmol). A yellow solid precipitated and the mixture was stirred under reflux for 18 h. After cooling to room temperature, the solid was filtered off, washed with dry hexane and dried under vacuum to afford a yellow solid. 0.1400 g. Yield 80%.

Crystals of **Zn2** suitable for X-ray diffraction analysis were obtained by slow evaporation of a deuterated dichloromethane solution of the complex.

Anal. Calcd. For $C_{34}H_{34}Cl_2N_4Zn{\cdot}H_2O{\cdot}$ (653.0): C 62.5, H 5.6, N 8.6; found C 62.4, H 5.1, N 8.5. ESI MS Calcd. For $C_{34}H_{34}ClN_4Zn$ *m/z*: 597.1763 $[M\text{-}Cl]^+$, found *m/z*: 597.1767 (100%).

^{1}H NMR (400 MHz, ppm, CD_2Cl_2) δ: 1.14 (t, 12 H, CH_3, J = 7.5 Hz), 2.70 (q, 8H, CH Et, J = 7.5 Hz), 7.11–7.16 (m, 6H, CH Ar), 8.18 (s, 2H, CH phen), 8.60 (d, 2H, CH phen, J = 8.3 Hz), 8.77 (d, 2H, CH phen, J = 8.3 Hz), 9.00 (s, 2H, CH═N). ^{13}C NMR (126 MHz, ppm, CD_2Cl_2) δ: 14.6, 24.6, 124.9, 125.5, 126.1, 128.0, 130.9, 140.3, 141.2, 147.9, 160.4. FTIR(cm^{-1},ATR): 2962 (m), 2928 (w), 2870(w), 1637 (m, C = N), 1617 (m, C = N), 1583 (m), 1564(m), 1505 (m), 1450 (m), 877(s), 798(s), 762

(s). Conductivity: 3.55·S.cm^2.mol^{-1} a T = 25 °C (CH_2Cl_2, 0.4.10^{-3} M).

2.1.3. Synthesis of dichloro(1,1′-(1,10-phenanthroline-2,9-diyl)bis(N-(3,4-dimethoxyphenyl)methanimine))zinc(II) (Zn3)

In a purged Schlenk tube under nitrogen, a mixture of $ZnCl_2$ (0.07 g, 0.51 mmol) and dry propanol (15 mL) was refluxed under stirring until the dissolution of the zinc salt. Then, **L3** was added (0.11 g, 0.23 mmol). A yellow solid precipitated and the mixture was stirred under reflux for 18 h. After cooling to room temperature, the solid was filtered off, washed with dry hexane and dried under vacuum to afford a dark pink precipitated. 0.1200 g. Yield: 81%.

Anal. Calcd. For $C_{30}H_{26}Cl_2N_4O_4Zn{\cdot}H_2O$·(660.9): C 54.5, H 4.3, N 8.5; found C 52.0, H 3.9, N 8.1. ESI MS Calcd. For $C_{30}H_{26}Cl_2N_4O_4Zn$ *m/z*: 641.0701 $[MH]^+$, 605.0934 $[M\text{-}Cl]^+$, found *m/z*: 605.0954 (100%), 641.0707 (18%). ^{1}H NMR (CD_2Cl_2, 400 MHz): 3.91 (s, 12H, OCH_3), 6.95 (2H, d, J = 8.4 Hz, Ar-H), 7.44 (2H, d, J = 8.4 Hz, Ar), 7.57 (2H, s, Ar), 8.07 (2H, s, phen), 8.50 (2H, d, J = 8.2 Hz, phen), 8.62 (2H, d, J = 8.2 Hz, phen), 9.44 (2H, s, CH═N). ^{13}C NMR (126 MHz, ppm, CD_3Cl) δ: 56.2, 106.4, 111.1, 117.2, 124.8, 127.4, 129.8, 139.5, 140.7, 140.9, 149.5, 150.1, 151.5, 152.9. FTIR(cm^{-1},ATR): 2965(w), 2837(w), 1609 (w, C = N), 1587(m), 1567(m), 1509(s), 1262(s), 1243(s), 1223(s), 1136 (s), 1121(s), 1017(s), 867(s), 857(s). Conductivity: 2.10·S.cm^2.mol^{-1} a T = 26.3 °C (DMF, 0.4.10^{-3} M).

2.1.4. Synthesis of dichloro(1,1′-(2,2′-bipyridine-6,6′-diyl)bis(N-(2,6-diisopropylphenyl)methanimine))zinc(II) (Zn4) [63]

In a purged Schlenk tube under nitrogen, a mixture of $ZnCl_2$ (0.039 g, 0.283 mmol) and dry 1-butanol (10 mL) was refluxed under stirring until the dissolution of the zinc salt. Then, **L4** was added (0.075 g, 0.142 mmol) and the reaction mixture was stirred at 100 °C for 18 h. After cooling to room temperature, the solvent was concentrated under reduced pressure and hexane was added to induce precipitation. The solid formed was filtered off, washed with dry hexane and dried under vacuum to afford a yellow solid. 0.063 g. Yield: 77%. The ^{1}H NMR data was consistent with literature values [63].

^{1}H NMR (400 MHz, ppm, CD_2Cl_2) δ: 1.15 (d, 24 H, J = 6.6 Hz), 3.15 (sept, 4H, CH(C*H*)$_3$, J = 6.6 Hz), 7.16 (m, 6H), 8.32 (m, 4H), 8.45 (m, 2H), 8.85 (m, 2H). ^{13}C NMR(126 MHz, ppm, CD_2Cl_2): δ 23.7, 27.9,121.7, 123.2, 124.0, 125.5, 126.6, 138.2, 141.5, 151.1, 156.2, 160.0. Conductivity: 4.23·S.cm^2.mol^{-1} a T = 25 °C (CH_2Cl_2, 0.4.10^{-3} M).

2.1.5. Synthesis of dichloro(N,N'-(2,2′-bipyridine-6,6′-diylbis(methylene))bis(2,6-diisopropylaniline))zinc(II) (Zn5)

In a purged Schlenk tube under nitrogen, a mixture of $ZnCl_2$ (0.07 g, 0.51 mmol) and dry propanol (17 mL) was refluxed under stirring until the dissolution of the zinc salt. Then, **L5** (0.123 g, 0.23 mmol) was introduced slowly and the mixture was stirred under reflux for 18 h. After cooling to room temperature, the solvent was removed under reduced pressure and hexane was added to induce the precipitation. The solid was filtered off, washed with cold hexane, and dried under vacuum to afford yellow crystals. 0.1034 g. Yield: 67%. Crystals of **Zn5** suitable for X-ray diffraction analysis were obtained by slow evaporation of a deuterated dichloromethane solution of the complex.

^{1}H NMR (400 MHz, ppm, CD_2Cl_2) δ: 1.14 (d, 24 H, J = 6.7 Hz), 3.09 (sept, 4H, CH(C*H*)$_3$, J = 6.7 Hz), 4.66 (m, 6H) 7.06–7.12 (m, 6H), 7.45 (d, 2H, J = 7.8 Hz), 8.06 (t, 2H, J = 7.6 Hz), 8.18 (d, 2H, J = 7.9 Hz). ^{13}C NMR (126 MHz, ppm, CD_2Cl_2) δ: 24.4, 28.2, 56.8, 119.6, 122.5, 123.9, 124.1, 137.8, 143.0, 144.2, 155.7, 158.6 ppm. FTIR (cm^{-1}, ATR): 3086 (w), (s), 2965 (s), 2948(m), 2879(m), 1637(m), 1600(m), 1586 (m), 1474(s), 1444(m), 1172(s), 1018(m), 796(s), 762(s), 732(m).

2.2. Catalysis

2.2.1. Standard procedure for the synthesis of cyclic carbonates

The catalytic tests were carried out in a 25 mL Parr reactor equipped with a magnetic stirrer and heated with a silicone oil bath. In a standard catalytic experiment, the reactor was charged with a solution of **Zn1**-**Zn5** complex (0.2 mol%) and TBAB (0.2–0.5 mol%) in the epoxide (20 mmol). The reactor was closed and purged with 2–3 bars of carbon dioxide. Then CO_2 was introduced to the desired pressure and the filled reactor was placed in the preheated bath. After 10 min of equilibration time, the stirring was switched on. After the desired reaction time, the reactor was cooled with an iced water-salt bath and gradually depressurized. The conversion of the epoxide was determined by ^{1}H NMR of the crude reaction using mesitylene as an internal standard. Since no by-products were detected by ^{1}H NMR we assumed that the conversion was, in fact, the NMR yield.

2.2.2. Semi-batch experiments

The first catalytic run was done as in the standard procedure using 30 mmol of **1b**, 0.06 mmol of TBAB (0.2 mol%) and 0.03 mmol (0.1 mol %) of **Zn1**. After the catalytic experiment, the reactor was cooled down with a liquid nitrogen bath and it was carefully depressurised. A sample of the crude was taken for ^{1}H NMR spectroscopy analysis using mesitylene as standard to determine the composition of the crude. Considering the conversion, fresh **1b** was added to reach 30 mmol, the solution was placed in the reactor and the catalytic reaction was run again as described in the standard procedure.

2.3. X-ray diffraction structures

Zn1 crystal structure data were collected at 100 (2) K using an Oxford Cryotream 700+ in a Bruker APEX DUO X-ray tube equipped with a CCD APEX II detector with Mo Ka radiation. Software for data collection and data reduction: APEX II and absorption correction SADABS Version 2008/1 Bruker-Nonius [64]. Software for data solution SIR2014 [65]. Software for data refinement SHELXL-2014/3 [66] under the shelXle [67] interface. **Zn2** and **Zn5** crystal structure's data were collected at 100 (2) K using an Oxford Cryotream 700+ in a Rigaku MicroMax-007HF Microfocus rotating anode X-ray tube equipped with a hybrid pixel detector PILATUS 200 K with Mo Ka radiation. Software for data collection, data reduction and absorption correction: CrysAlisPro 1.171.40.35a [68] Empirical absorption correction using spherical harmonics, implemented in SCALE3 ABSPACK [68] scaling algorithm. Software for data solution SIR2019 [65]. Software for data refinement SHELXL-2018/3 [66] under the shelXle [67] interface. Crystallographic data are collected in Tables S1, S3–S11 (Supplementary Information).

2.4. Computational methods

The geometry optimizations and frequency calculations have been carried out using the DFT method as implemented in Gaussian 16. B3LYP functional was chosen to be used in all calculations due to its good performance in similar systems. The Solvation Model Based on Density (SMD) was used to describe the reaction media as a polarizable continuum. In the experimental setup, the solvent is the reactant epoxide. For the calculations we used 2-butanol as the solvent, given that this one is in the Gaussian library and has similar properties to **1b**, with a dielectric constant ε = 15.94 (ε = 16 for **1b**) and a refractive index, η_D = 1.397 (η_D = 1.366 for **1b**) [69].

Gibbs free energy (G) and frequencies (that confirmed that the structures found were energy minima) were also calculated.

An exploratory study was performed to determine the most appropriate computational model (or level of calculation) to be used looking for a balance between the accuracy of results and computational costs. Several calculations with decreasing levels of accuracy (using smaller basis sets and simpler computational methods) were performed on a model system (**ZnH**, *i.e.* R^1=R^2=H, Scheme 3) and compared with a benchmark computational model performed at a high level, *i.e.* cam-b3lyp/aug-cc-pVTZ with Grimme's D3BJ empirical dispersion correction (nomenclature: *density-functional/basis-set*), to identify the cheapest

level of calculation which results agreed with the chosen benchmark. The results of this study are shown in Tables S12 and S13 of the Supplementary Information.

As a result of this analysis, we have used B3BYP/6–31+*G*(d,p) for geometry optimizations and frequency calculations and CAM-B3BYP-D3BJ/aug-cc-pVDZ for energy calculations (represented as B3BYP/6–31+*G*(d,p)//CAM-B3BYP-D3BJ/aug-cc-pVDZ computational level). To obtain Gibbs free energies, the entropic term obtained from the frequency calculation performed at the former computational level was added to the energies obtained at the latter one. All the results reported in the main text of the paper were obtained following this computational strategy (with the correction to the free energy explained further down) unless otherwise explicitly stated.

Another preliminary study focused on catalyst **Zn1** was performed to explore the experimental model. We wanted to know which of the different isomers and/or conformations of the catalysts corresponded to lower energy species. The information derived from this study would allow us to identify the ones expected to be present in the experimental systems to reduce the number of species to be computed in the other catalysts of the series studied. The initial free energy differences (ΔG) obtained (in Table S18 of Supplementary Information) showed that the energy differences were very small in some cases (less than 1 kcal mol^{-1}). Unfortunately, they are of the same order as the expected error in the calculation of G, derived from the error of the entropic contribution calculated based on the frequencies, which show a typical uncertainty of 20 cm^{-1}. For this reason, to obtain more reliable results, a correction proposed by Grimme [70] (where the low-lying vibrational modes are treated by a free-rotor approximation) was applied to recalculate the free energies, considering room temperature. The values of ΔG shown and discussed in the next section contain this correction.

3. Results and discussion

3.1. Syntheses of ligands L1-L5 and complexes Zn1-Zn5

1,10-Phenanthroline bis(imine) **L1-L3** (Scheme 3) and 2,2′-bipyridine bis(imine) **L4** ligands were prepared by condensation of 1,10-phenanthroline-2,9-dicarbaldehyde [58] and 6,6′-diformyl-2,2′-bipyridine [61,63,71] with the corresponding aniline derivative as previously reported [59,60,63] (Scheme 3). The 2,2′-bipyridine bis(amine) ligand **L5**, was prepared by reduction of **L4** with $LiAlH_4$ as reported for related imines [72]. The reaction of the ligands **L1-L3** and **L5** with anhydrous $ZnCl_2$ in 1-propanol led to the corresponding Zn(II) complexes, **Zn1-Zn3** and **Zn5** (Scheme 3) in good yields (64–81%). Complex **Zn4** was previously reported in the literature and was prepared accordingly [63]. In the case of **Zn1**, the complex was also prepared by a one-pot direct reaction of 1,10-phenanthroline-2,9-dicarbaldehyde [58] with the 1,5-diisopropylaniline and anhydrous $ZnCl_2$ in dry propanol under reflux but the yield was lower (*ca* 20%) than in the two-steps synthesis. The new complexes **Zn1-Zn3** and **Zn5** were characterized by high-resolution electrospray time of flight mass spectrometry (HRMS ESI-TOF), elemental analysis and FTIR and NMR spectroscopies. X-ray diffraction structures were obtained for **Zn1**, **Zn2** and **Zn5**.

The ESI-TOF mass spectra of the new complexes **Zn1-Zn3** and **Zn5** presented peaks at *m/z* corresponding to $[M\text{-}Cl]^+$ fragments (Experimental Section) and the elemental analysis were in concordance with [Zn(**L1-L5**)Cl_2] formula. Confirmation of the neutral nature of the coordination entities was obtained by the low values of the conductivity in solution (values < 5 $S{\cdot}cm^2{\cdot}mol^{-1}$). Evidence of the ligand coordination was obtained by the FTIR and NMR spectra. For **Zn1**, 2D NMR COSY, HMBCAD and HSQCAD experiments allowed the assignment of the signals (Figs. S13–S16). In the FTIR spectra of the imine complexes, signals at *ca* 1635 cm^{-1} attributed to the stretching C = N vibration confirm the presence of the coordinated ligand. These signals slightly shifted (2–3 cm^{-1}) to higher frequencies indicating a poor backbonding from the metal. It could not be distinguished if both imine groups were coordinated since there was overlapping with signals from the phenanthroline skeleton (1600–1400 cm^{-1}) [73]. Neither the ^1H NMR spectra were useful in determining the denticity of the ligand. The spectra presented a symmetrical pattern in which the phenanthroline and bipyridine proton's signals appear as equivalents in the δ 7.4–8.9 ppm region. The aniline proton signals are observed in the δ 7.0–7.5 ppm region and the CH═N imine signal can be detected in the δ 8.4–9.0 ppm interval for the **Zn1-Zn4** complexes. The ^1H NMR spectrum of **L5** does not show the CH═N signal at δ 8.40 ppm and a new singlet at δ 4.26 ppm corresponding to the new methylene group -CH_2-NH confirms the reduction of the imine. The ligand's signals for **Zn1-Zn5** suffer a shielding to higher chemical shifts confirming the coordination to the metal centre. Furthermore, only one imine signal is observed in the ^1H NMR spectra of **Zn1-Zn4** although, as will be discussed in the next section, the X-ray diffraction structure of **Zn1** and **Zn2** indicates that the ligand is acting as tridentate coordinating to the metal through the phenanthroline and one imine. This suggests that a fluxional behaviour (Scheme 4) can take place in solution as observed for related complexes [32]. According to these data, we assumed that the bis(imine) complexes **Zn1-Zn4** had the same structure. The computational relative stability calculations agree with this proposal too (see Section 3.3).

3.2. X-ray structure of Zn1, Zn2 and Zn5

Yellow crystals of the phenanthroline diimine derivatives **Zn1**, **Zn2** and **Zn5** suitable for X-ray diffraction analysis were obtained from deuterated chloroform and deuterated dichloromethane solutions. The ORTEP diagrams for **Zn1** and **Zn5** are shown in Fig. 1 and selected bond distances and angles are listed in Table S2. The structures of **Zn1** and **Zn2** are similar, so only **Zn1** will be discussed here, while the structural information on **Zn2** can be found in Supplementary Information. **Zn1** is a neutral molecule with a five-coordinated Zn metal centre bonded to two chloride ligands and one **L1** acting as tridentate κ3 *N,N,N*'-donor with one of the imino groups non-coordinated (*exo*) giving an overall *endo-exo* configuration of the imine groups. The metal centre coordination unit has a distorted pentacoordinate geometry. The distortion described by the τ-factor (0.31) points to a distorted square-pyramidal geometry (τ = 0 for a perfect square-pyramidal geometry while τ = 1 for a trigonal bipyramidal one) [74]. The Zn-N and Zn-Cl bond distances are in the range of the ones reported for the related complexes containing **L1** [52,71,75–77]. The Zn-N3 distance (2.052(3) Å) corresponding to the central donor atom in the tridentate ligand (Fig. 1) is significantly shorter than the Zn-N2 and Zn-N4 bond lengths (2.309(4) and 2.348(4) Å respectively) like the ones reported for related complexes [75,76,78]. The imine C = N bonds retain their double bond character [63], but the relative longer distance in the coordinate imine indicates a weak back donation from the metal confirming the IR data. The relative orientation of the imine groups is in both cases *trans* and the aryl substituents of the imino groups are *ca* ortogonal to the plane defined by the N-coordinated ligand. The relative disposition of the two aryl moieties is slightly disrotatory (not parallel aromatic planes) as reported for a similar Zn(II) complex [63].

Instead, the bipyridine-bis(amine) zinc complex **Zn5** presents a four-coordinate structure with pseudo-tetrahedral geometry in which **L5** acts as a bidentate ligand with the free amine groups located outside the coordination sphere (*exo*), similar to reported examples [63]. The relative positions of the aryl and pyridyl groups are in a disrotatory conformation. The higher flexibility of the bipyridyl structure and the steric repulsion created by the two *orto iso*propyl substituents may account for the formation of the lower coordination number isomer. Nevertheless, to get inside the reasons for these structural differences we decided to undertake computational calculations on the relative stability of the different possible structures.

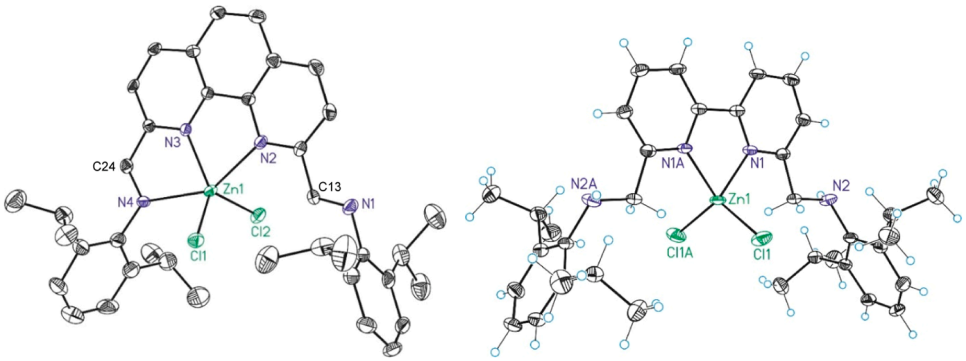

Fig. 1. ORTEP drawing of complex of Zn1 (left) and Zn5 (right). All hydrogen atoms and solvent molecules are omitted for clarity. Thermal ellipsoids are drawn at the 50% probability level.

3.3. Computational results

To identify the most probable isomers and conformations of the catalysts, a preliminary analysis was performed with two different complexes: with a model containing the unsubstituted aniline derivative **ZnH** (R^1=R^2=H, Scheme 3) and with **Zn1** (Scheme 3).

The first characteristic that will distinguish different isomers is the orientation of the imine (amine in **Zn5**) groups relative to the central Zn atom. We observed that the *exo* relative position of the imine (or amine) precluded the coordination of the nitrogen with the central Zn atom. For this reason, a coordination number (CN) 6 (represented as **ZnL/6**) is only possible in *endo-endo* orientation of these groups while *endo-exo* isomers gave place to species **ZnL/5** with CN = 5 (see for example atoms N4 and N1 in the ORTEP drawing of complex **Zn1** in Fig. 1) and *exo-exo* ones to CN = 4, **ZnL/4** (atoms N2A and N2 in the ORTEP drawing of complex **Zn5** in Fig. 1). Nevertheless, for the more flexible bipyridine derived ligand **L5**, the imine (amine) N atom in *endo* conformation can be located far from the Zn atom and in fact some stable isomers with CN=4 and *endo* orientation of the imine (amine) groups were located. For each of those species, the *cis/trans* isomerism around the imine double bond was also considered, as well as the similar *syn/anti* conformers that can be described for amine groups. On top of this, the possible relative orientation of the planes of the phenyl substituents when they are not parallel, conrotatory (**ZnL$_{con}$**) and disrotatory (**ZnL$_{dis}$**), were also taken into account, but given the small energy differences found between them, only one of this dispositions will be considered in the following. Some examples of these possible conformers are shown in Fig. 2. The relative energies of the isomers explored are shown in Supplementary Information (Section 4).

As a whole, the most stable isomer for both **ZnH** and **Zn1** was that with CN=5 and *endo-trans/exo-trans* conformation (Fig. 3a), although the energy difference for isomers with CN=5 and CN=4 conformation was small (2.8 kcal mol^{-1} and 2.6 kcal mol^{-1} for **ZnH** and **Zn1** respectively, Tables S14 and S16).

We then studied the zinc bipyridine derivatives with the iPr substituent in the aryl group **Zn4** and **Zn5**. Given the results for **ZnH** and **Zn1** complexes, only the predicted most stable species with CN 4 and 5 were taken into account in this part of the computational study. The relative free energies obtained for these systems are shown in Table S17. For the bis(imine) complex the most stable isomer had coordination number 5, **Zn4/5,** with a *trans* relative disposition of the imine groups. Consequently, we propose that the bis(imine) Zn(II) complex with bipyridine skeleton **Zn4** has the same structure as the phenanthroline derivatives **Zn1** and **Zn2** (geometry shown in Fig. 3b). Instead, for the bipyridine bis(amine) derivative **Zn5**, the most stable isomer in solution is the one with coordination number 4 and an *exo-anti/exo-syn* relative disposition of the aryl aniline groups (Fig. 3c).The five-coordinated and the other four-coordinated isomers are less stable in *ca* 4 kcal mol^{-1}.

To check the reliability of these conclusions, the geometries obtained computationally for isomers **Zn1** and **Zn5** were compared with the X-ray structures obtained. The most stable isomer computed for **Zn1** is in agreement with the structure determined experimentally, **Zn1/5**$_{endo\text{-}trans/exo\text{-}trans}$. Fig. 4 shows together, for comparative purposes, the X-ray diffraction structure of this complex (left) with its computationally optimized geometry (right). At first sight, the most evident difference is the angle of the planes of the aryl substituents. Nevertheless, this is not a crucial difference given that, as seen in the preliminary conformational study, this geometric parameter does not change significantly the energy of the complex. Comparing selected parameters of these geometries (Table S2), We observe that the bond distances and angles are in general in good agreement, with errors up to 7% for distances and 3% in angles, except for one of them that surprisingly shows a 38% of discrepancy. It must not be forgotten that the computational geometry has been simulated in solution while the experimental structure comes from a crystal environment.

For **Zn5**, the computational more stable structure agrees with the tetrahedral geometry determined by X-ray diffraction data although in this case the **Zn5/4**$_{exo\text{-}anti/exo\text{-}anti}$ isomer was observed in the crystalline

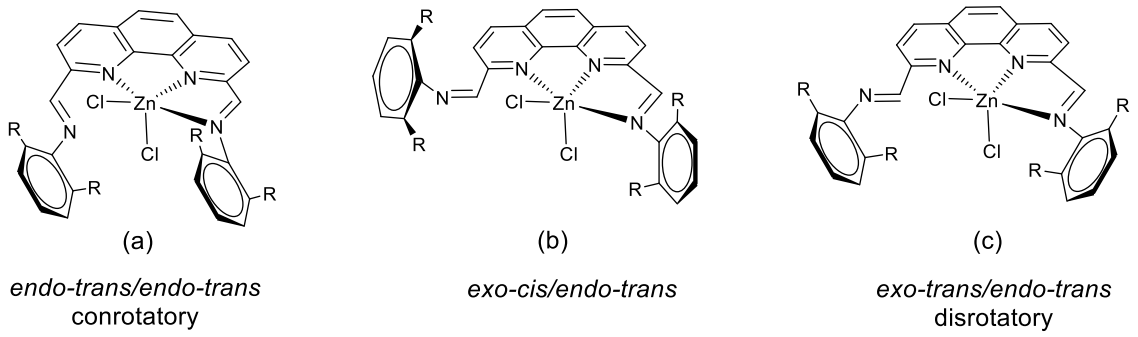

Fig. 2. Examples of possible conformers of ZnL/5: (a) *endo-trans/endo-trans* conrotarory, (b) *exo-cis/endo-trans* and (c) *exo-trans/endo-trans* disrotatory.

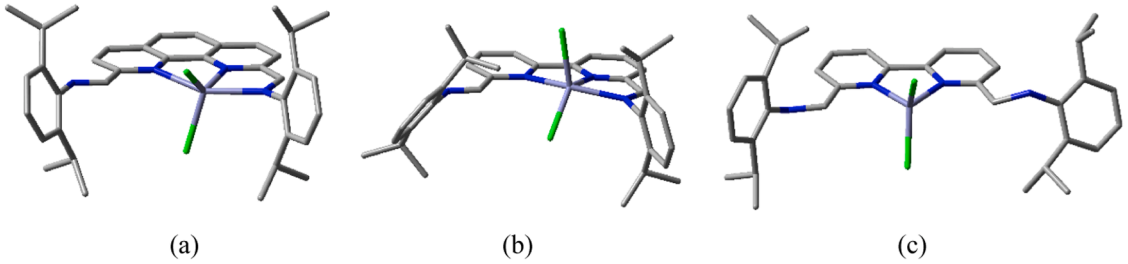

Fig. 3. Most stable isomers of complexes (a) *endo-trans/exo-trans*-Zn1/5, (b) *endo-trans/exo-trans*-Zn4/5 and (c) *exo-anti/exo-syn*Zn5 obtained computationally. H atoms omitted for clarity. Colour code: Zn light blue; Cl green; C grey; N dark blue.

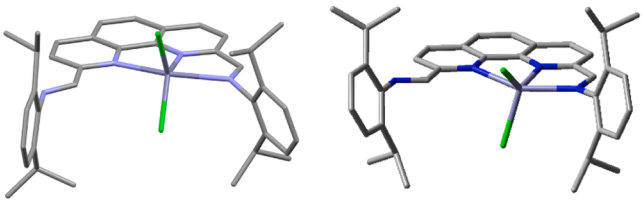

Fig. 4. X-ray diffraction structure of this complex (left) and computationally optimized geometry (right) of Zn1. H atoms omitted for clarity. Colour code: Zn light blue; Cl green; C grey; N dark blue.

phase while computations predict the *exo-anti/exo-syn* to be more stable. Packing effects in the crystal or interactions with the solvent in solution may affect differently the different stereoisomers of the **Zn5** complex. Nevertheless, geometrical parameter differences (shown in Table S2) are small (up to 6.5% errors in distances and only up to 3% in angles) so the agreement can be considered good.

In view of the good prediction of the geometries for compounds **Zn1** and **Zn5** and the results obtained for **Zn4**, we propose that the bis(imine) Zn(II) complex with bipyridine skeleton **Zn4** has the same structure as the phenanthroline derivatives **Zn1** and **Zn2**.

3.4. Catalysis

3.4.1. Reaction conditions optimization

The catalytic activity of the zinc phenanthroline-bis(imine) (**Zn1-Zn3**), bipyridine-bis(imine) (**Zn4**) and bipyridine-bis(amine) (**Zn5**) complexes in the cycloaddition of CO_2 to epoxides to form the corresponding cyclic carbonates (Scheme 1) was studied. First, it was examined the cycloaddition of CO_2 to the benchmark substrate 1,2-epoxyhexane (**1a**, Scheme 1) with the complex **Zn1** at a catalyst loading of 0.1 mol% using the epoxide as a solvent.

The catalytic activity of **Zn1** was very modest under the conditions of 30 bar of CO_2 and 80 °C (only 9% yield after 20 h reaction time, entry 1, Table 1). Most probably, the chloride coordinated to the zinc centre is not dissociating enough free ions to act as a nucleophile to initiate the reaction through the ring opening of the epoxide. Indeed, **Zn1** in solution presents a low conductivity corresponding to a neutral molecular species. Thus, we decided to add the commonly used nucleophile (Nu) tetrabutylammonium bromide (TBAB) [13] in a 1:2 molar ratio with respect to **Zn1**. The binary system **Zn1**/TBAB (1:2) under 10 bar of CO_2 at 80 °C increased the conversion up to 61% (entry 2, Table 1) corresponding to an average turnover frequency (TOF) of 206 h^{-1}. Only the cyclic carbonate product was detected by ^{1}H NMR (Fig. S29, Supplementary information). Under the same conditions, TBAB, which is known to be an active catalyst for this transformation [13], provided lower conversion (entry 3, Table 1), what confirms that the complex and the nucleophile are working cooperatively. Increasing the **Zn1**/TBAB ratio to 1:5 the conversion increased up to 73% (entry 4, Table 1), but in this case the reference experiment using only TBAB provided a similar conversion (entry 5, Table 1). A decrease in temperature to 60 °C also produced a drop in conversion (entry 6, Table 1).

To facilitate the dissociation of the chloride from the complex to participate in the ring opening of the epoxide, we added a soluble salt sodium tetrakis-[3,5-*bis*(*trifluormethyl*)*phenyl*]borate (NaBArF), which contains a low coordinating anion. Using as catalyst **Zn1** in the presence of 2 equivalents of NaBArF the reaction was blocked (entry 7, Table 1), probably because the NaCl thus formed is not soluble in the reaction media. Neither the **Zn1**/2NaBArF system in the presence of TBAB was active (entry 8, Table 1) probably due to the same reason.

To confirm this hypothesis, the species formed in the mixture of **Zn1** with NaBArF, TBAB and **1a** were monitored by ^{1}H and ^{19}F NMR. When two equivalents of NaBArF were added to a suspension of **Zn1** (0.02 mmol) in CD_2Cl_2 (2 mL) the dissolution of **Zn1** was observed together with the formation of turbidity probably corresponding to NaCl precipitation. The ^{1}H NMR of this mixture (Figs. S31 and S32) showed a shift in the signals corresponding to the coordinated **L1** confirming that a new complex formed. Since the ^{19}F NMR spectra showed a signal at δ −62.84 ppm corresponding to free NaBArF (Fig. S33), then, presumably [Zn(**L1**)][BArF] formed. Subsequent addition of 2 equivalents of TBAB produced a shift in the ligand signals and partial precipitation of a yellow solid, which may be related to Br^- coordination to form [Zn(**L1**)Br]$^+$ or [Zn(**L1**)Br_2]. Further addition of 5 equivalents of 1,2-epoxyhexane did not produce any change in the spectra nor was it observed a shift

Table 1
Catalytic activity of Zn1 and TBAB in the cycloaddition of CO_2 to 1,2-epoxyhexane (1a).[a]

Entry	**Zn1**/Nu	**Zn1**/Nu (mol%)	**Zn1**/Nu molar ratio	P (bar)	T (°C)	t (h)	Conv[b] (%)	TOF average[c] (h^{-1})
1	**Zn1**/-	0.1/-	1/0	30	80	20	9	4
2	**Zn1**/TBAB	0.1/0.2	1/2	10	80	3	61	206
3	-/TBAB	-/0.2	0/1	10	80	3	45	–
4	**Zn1**/TBAB	0.1/0.5	1/5	10	80	3	73	–
5	-/TBAB	-/0.5	0/5	10	80	3	75	–
6	**Zn1**/TBAB	0.1/0.2	1/2	10	60	3	27	90
7	**Zn1**/-/NaBArF	0.1/-/0.2	1/0	10	80	3	–	–
8	**Zn1**/TBAB/NaBArF	0.1/0.2/0.2	1/2/2	10	80	3	–	–

[a] General conditions: 20 mmols of **1a**, catalyst 0.02 mmol (0.1 mol%), TBAB (0.04 mmol, 0.2 mol%).
[b] Conversion determined by ^{1}H NMR using mesythylene as internal standard.
[c] TOF turnover frequency = mols of **1a** converted per mol of Zn complex per hour.

of the epoxide signals, which indicates that the epoxide does not interact with the zinc complex. ^{19}F NMR did not show any evidence of $BArF^-$ coordination in any of the experiments. Therefore, it was confirmed that the addition of NaBArF favored the dissociation of the chlorine ligands that were replaced by bromine in the presence of TBAB forming an inactive species.

To assess the influence of carbon dioxide pressure we choose the molar ratio **Zn1**/TBAB of 1:2 and 80 °C reaction temperature. The results are represented in Fig. 5. We observed that the increase of the pressure from 10 bar to 30 bar resulted in a drop in epoxide conversion. This behaviour may be related to a decrease in the solubility of the catalyst in the CO_2 enriched epoxide-carbonate mixture media. Decreasing the pressure to 1 bar the system was still active with an initial TOF of 53 h^{-1} (Fig. 5) and a high conversion (77%) was obtained after 24 h (Fig. 5). Remarkably, under these conditions, the reference experiment using only TBAB as a catalyst produced only 26% of conversion, then an increase of *ca* 50% in conversion was obtained by combining the **Zn1** complex with TBAB, confirming the positive effect of using the zinc complex and the nucleophile together.

Once the optimized conditions were established, the effect of the environment of the Zn(II) centre was studied by comparing the activity of the catalytic systems **Zn1-Zn5**/TBAB under the same reaction conditions. The TOF values obtained at 3 h reaction time are shown in Fig. 6. The catalytic systems **Zn2**/TBAB and **Zn3**/TBAB provided lower conversion in the carbonate than the isopropyl derivative **Zn1**/TBAB (Fig. 6). Moreover, the complexes with a more flexible bipyridine skeleton, **Zn4** and **Zn5**, produced lower conversion than the phenanthroline analogs under the same conditions (Fig. 6). Interestingly, the amine derivative **Zn5** produced twice the conversion of the analogue zinc bis (imine) system. In this case, the free amine groups may participate in the activation of the CO_2 as observed with other amines [79].

The initial TOF at 80 °C and under 10 bar of pressure was measured with the most active system of this series **Zn1**/TBAB at lower catalytic loading giving an averaged TOF of 565 h^{-1} at 38% conversion (Fig. 6). A comparison with data obtained with related zinc-based systems is shown in Table 2. It is difficult to compare the results because there is not enough data at the initial stage of the reaction. Nevertheless, the averaged TOF has been estimated when it was not reported. For the systems combining simple Zn(II) salts with tetrabutyl ammonium halides the activities obtained under mild conditions are modest (entries 1–3, Table 2, averaged TOF 6–64 h^{-1}) and only under high pressure (80 bar, entry 4, Table 2) the activity reached a high TOF (966 h^{-1}). The **Zn1**/TBAB catalytic system provided an averaged TOF of 32 h^{-1} for the

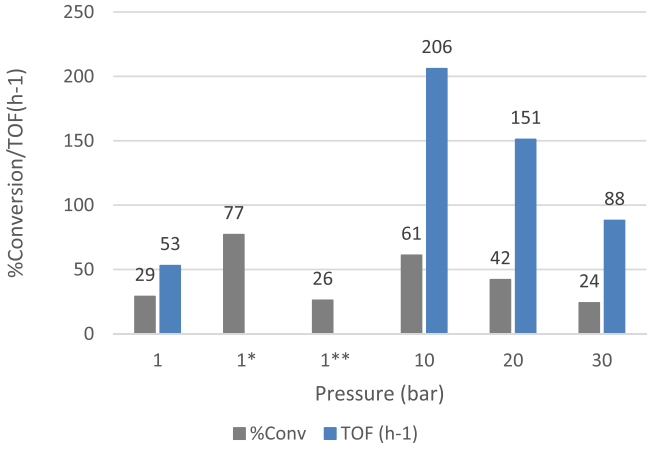

Fig. 5. Effect of pressure on the cycloaddition of CO_2/1a. Reaction conditions: 20 mmols of 1a, Zn1t 0.02 mmol (0.1 mol%), TBAB (0.04 mmol, 0.2 mol%), temperature: 80 °C, 3 h. Conversion and TOF determined by ^1H NMR using mesitylene as internal standard.*Zn1/TBAB (0.13/0.2 mol%), 24 h. **Only TBAB (0.2 mol%), 24 h.

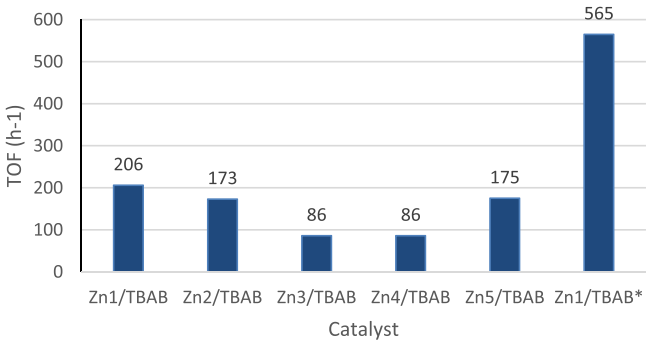

Fig. 6. Cycloadition of CO_2 to 1a using Zn1-Zn5/TBAB as catalytic system. General conditions: 20 mmols of EPH, catalyst (0.1 mol%), TBAB (0.2 mol%); 10 bar CO_2, 80 °C; 3 h TOF determined by ^1H NMR using mesythylene as internal standard. * Zn1 0.066 mol%/TBAB (0.1 mol%), 30 bar CO_2; 1 h.

epoxide **1a** at atmospheric pressure (entry 13, Table 2). **Zn1**/TBAB is a better catalytic system than our previously reported Zn(II) catalyst with NN'O-donor ligands (**C1**), which showed modest TOF for **1a** (entry 5, Table 2) and it decomposed after the catalytic reaction. Considering the Zn catalysts with N-donor ligands **C2-C6** (entries 6–10, Table 2), **Zn1**/TBAB presents a higher catalytic activity even at low pressure (TOF 206 h^{-1} at 10 bar) although is remarkable the robustness reported for system **C4**/TBAI which remains active for 4 days and for **C6**/TBAI which allows recycling the catalyst in 5 runs with small loss of conversion.

3.4.2. *Scope and stability of the catalytic system*

The scope of the reaction was analysed with other terminal and internal benchmark epoxides (**1b-1f**, Scheme 1) at 10–20 bars of CO_2 pressure, 80 °C using the **Zn1**/TBAB catalytic system (Table 3). Cyclic carbonates were also obtained as the only products detected by ^1H NMR. The averaged TOF obtained in the cycloaddition of CO_2 to propylene oxide and 1,2-epoxy-3-phenoxypropane (**1b** and **1e**, entries 1 and 2, Table 3) was slightly higher than for **1a** as expected due to the higher steric hindrance of the later. Slightly lower TOF were obtained in the cycloaddition of CO_2 to epichlorohydrin and styrene oxide (**1c** and **1d**, entries 3 and 4, Table 3). For a disubstituted more hindered epoxide such as **1f**, the conversion was lower as expected but, nevertheless, a significative TOF of 72 h^{-1} was achieved). In this case only the *cis*-**2f** was detected by ^1H NMR.

The stability of the catalytic system **Zn1**/TBAB under the reaction conditions was studied by performing the reaction in a semi-batch mode with **1b**. To do so, after 6 h catalytic run, the pressure was released, a sample for ^1H NMR analysis was taken and fresh **1b** was added to reach the initial amount. The sample was repressurised and the reaction was run again. The analysis of the crude obtained in these experiments is represented in Fig. 7. The analysis by ^1H NMR of the contents after each run showed a constant value of *ca* 82–84% of carbonate **2b** in the crude. Taking into consideration that fresh **1b** was added in each run to achieve the initial value of 30 mmol and the carbonate accumulated in the crude, the composition of the crude indicates that the catalyst was stable and active in the consecutive runs. Indeed, at the end of one of the catalytic experiments **Zn1** complex was partly recovered by precipitation after the addition of EtOH and the ^1H NMR spectra confirmed the presence of the complex (Fig. S30, Supplementary Information). Nevertheless, the partial conversion for each run decreased from 84 to 57% what may be related to the dilution effect caused by the **2b** accumulated in the reaction media although the partial decomposition of the Zn complex in the reaction media cannot be ruled out.

3.4.3. *Mechanistic proposal*

The cycloaddition results obtained with **Zn1-Zn5**/TBAB systems, computational stability calculations and previously reported data conduces to propose a cooperative mechanism between the Zn complex and

Table 2
Zn(II) based catalytic systems for the cycloaddition of CO_2 to epoxides[e].

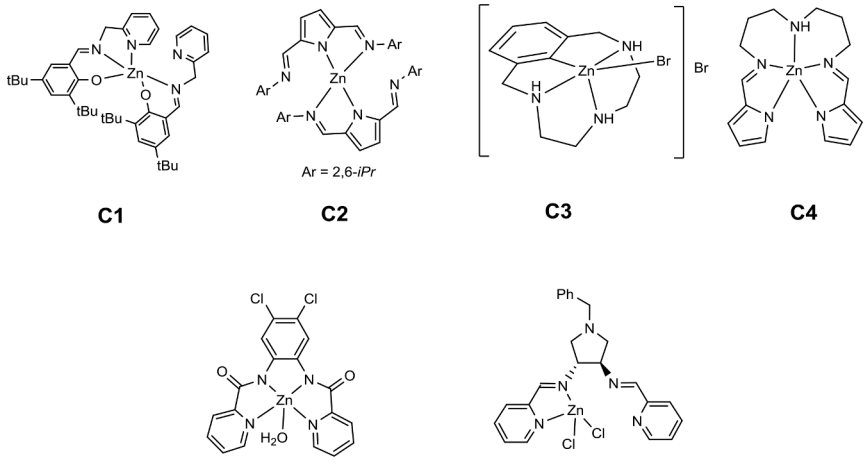

Entry	Cat/Co-cat (mol%)	Epoxide[a]	P(bar)[b]	T (°C)	t(h)	Conv/Y[c] (%)	TOF[d] (h^{-1})	Refs.
1	$ZnCl_2$/TBAI (4/16)	**1b**	1–1.2	r.t.	3.5	90/-	64[d]	[80]
2	$ZnCl_2$/TBAI (0.2/0.8)	**1c**	1–1.2	r.t.	24	37/-	8[d]	[80]
3	$ZnCl_2$/TBAI (0.2/0.8)	**1d**	1–1.2	r.t.	24	27/-	6[d]	[80]
4	$ZnBr_2$/TBAI (0.14/0.56)	**1d**	80	80	0.5	69/-	966[d]	[81]
5	**C1**/TBAB (0.14/0.2)	**1a**	50	80	24	87/-	25[d]	[32]
6	**C2**/TBAB (2.5/5)	**1a**	1	25	18	-/79	1.76	[82]
7	**C3/-** (0.5/-)	**1a**	8	125	3	99/93[d]	66	[56]
8	**C4**/TBAB (1/3)	**1a**	10	100	18	-/87	4.8[d]	[57]
9	**C5**/TBAB (0.2/0.2)	**1a**	50	80	20	40/-	10[d]	[49]
10	**C6**/TBAI (0.025/0.125)	**1a**	30	80	16	60	150[d]	[51]
11	**Zn1**/TBAB (0.066/0.1)	**1a**	30	80	1	61/-	565	This work
12	**Zn1**/TBAB (0.1/0.2)	**1a**	10	80	3	38/-	206	This work
13	**Zn1**/TBAB (0.13/0.2)	**1a**	1	80	24	77/-	32	This work

[a] Epoxides: see Scheme 1.
[b] Initial pressure.
[c] Conversion (Conv) and yield (Y).
[d] Averaged TOF (h^{-1}).
[e] Estimated from reported data; r.t. = room temperature.

Table 3
Catalytic activity of **Zn1**/TBAB in the cycloaddition of CO_2 to epoxides **1b-1f**.[a]

Entry	Epoxide	Conv.(%)[b]	TOF (h^{-1})[c]
1	**1b**	82	208
2	**1e**	84	228
3	**1c**	69	176
4	**1d**	58	145
5[d]	**1f**	28 (*cis*-**2f**)	72

[a] Reaction conditions: 20 mmols epoxide (**1b-1f**); **Zn1** 0.026 mmol (0.13 mol %); TBAB 0.04 mmol, (0.2 mol%), 10 bar, 80 °C, 3 h.
[b] %Conversion in the cyclic carbonates (**2b-2f**).
[c] Averaged TOF (h^{-1}).
[d] 20 bar.

TBAB (Scheme 5). In the first step, the Zn complex may activate the epoxide by coordination. In the case of imine pentacoordinate complexes (**Zn1-Zn4**, Scheme 5a), the addition of the epoxide is not favoured since it leads to a less stable hexacoordinate species, according to the DFT calculations. The relative stability of the hexacoordinate species with respect to the pentacoordinate ones depends on the substituents in the *orto* position; the difference of ΔG for the unsubstituted complex **ZnH/6** is 2.95 kcal/mol (Table S14) while for **Zn1/6** it is 6.43 kcal/mol (Table S16), so we can assume that hexacoordinated species are relatively more unstable than pentacoordinate ones for bulkier *orto* substituents. If the coordination of the epoxide was the rate determining step (rds), then, the more unstable the intermediate, the less active the

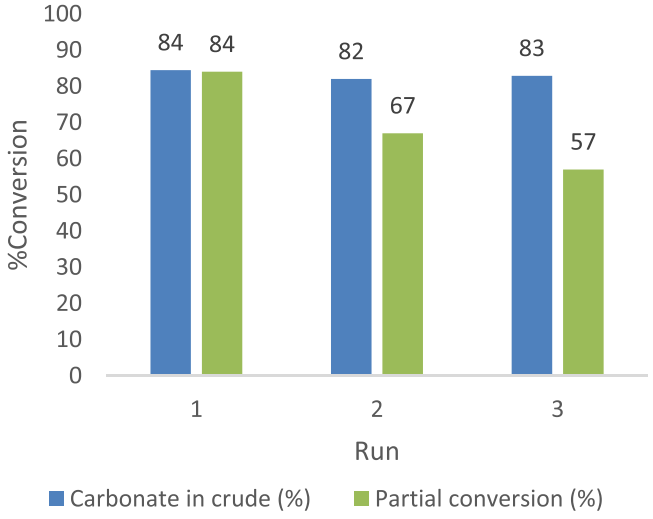

Fig. 7. Conversion in 2b obtained using Zn1/TBAB catalytic system. Reaction conditions: 30 mmols 1b; Zn1 0.03 mmol (0.1 mol%); TBAB 0.06 mmol, (0.2 mol%), 10 bar, 80 °C, 6 h.

system. This fact does not agree with the experimental observations that show an increase of activity when the steric hinderance of the substituent of the aniline in the *orto* position increases, so the initial assumption

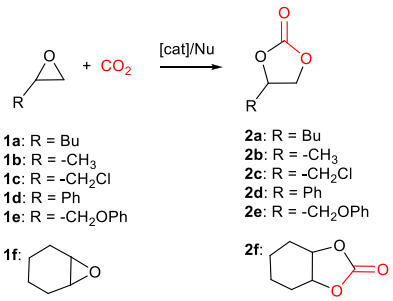

Scheme 1. Cycloaddition of CO_2 to selected epoxides to form cyclic carbonates.

can be discarded.

On the other hand, if the dissociation of the cyclic carbonate was the rds, it will be favoured in complexes with preference for low CN and high steric hinderance. This hypothesis is in fact in agreement with the

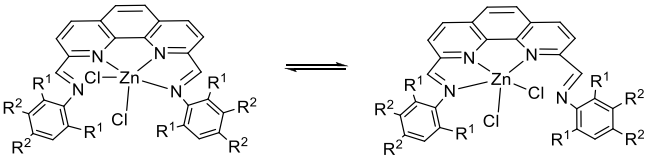

Scheme 4. Fluxional process proposed for Zn1-Zn4 in solution.

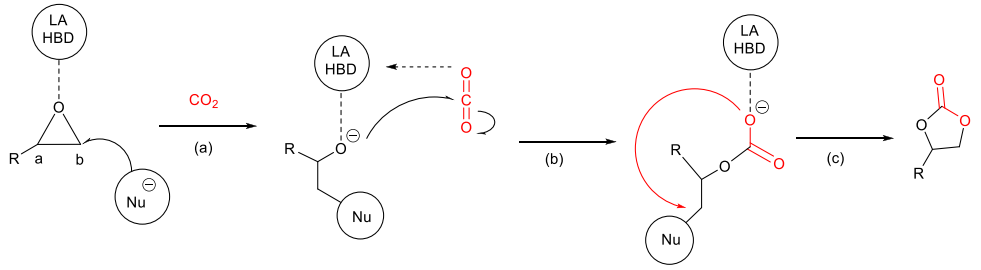

Scheme 2. Generally accepted mechanism for the synthesis of cyclic carbonates by a binary system LA or HBD/Nu. Based on Martin et al. [39].

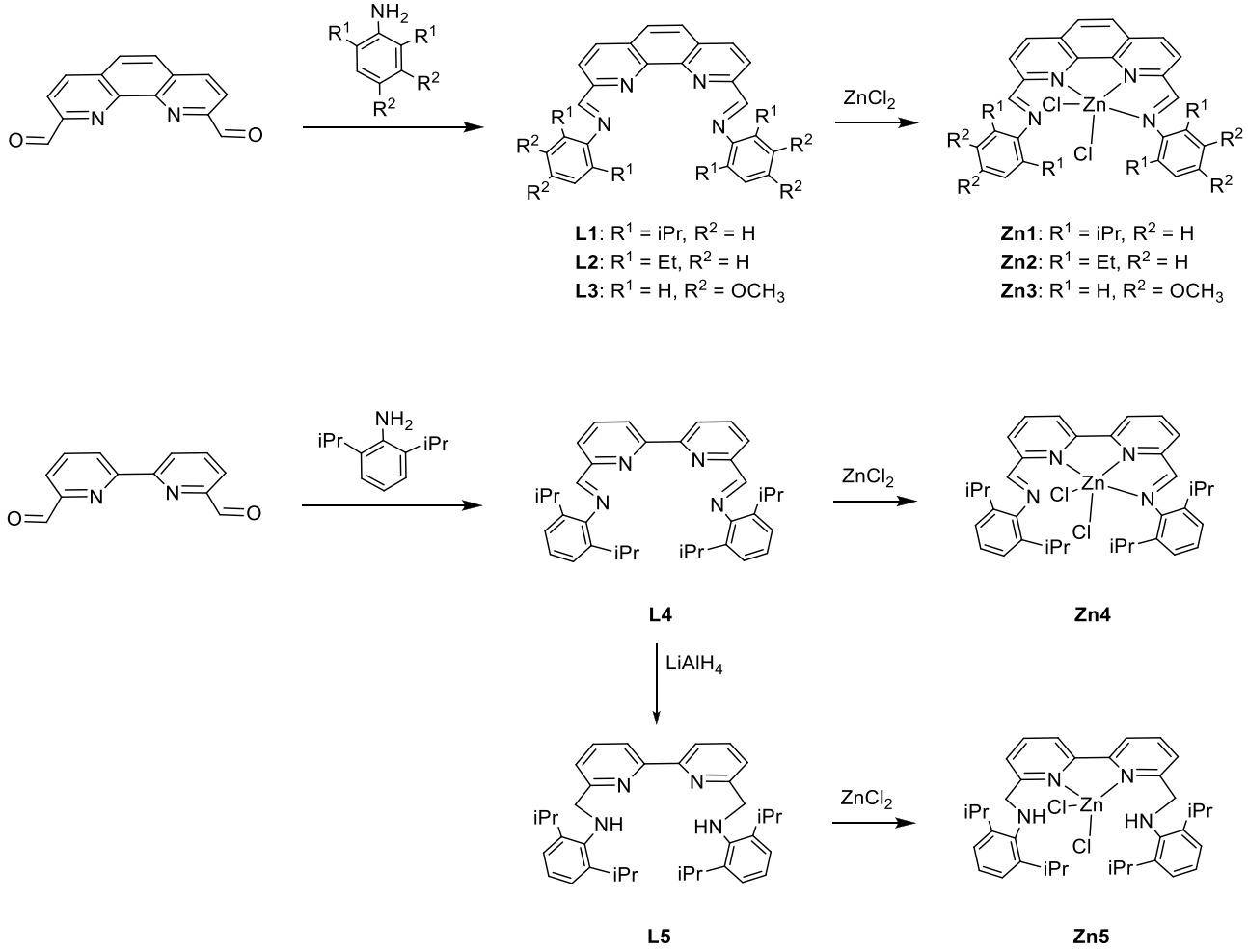

Scheme 3. Synthesis of ligands L1-L5 and complexes Zn1-Zn5.

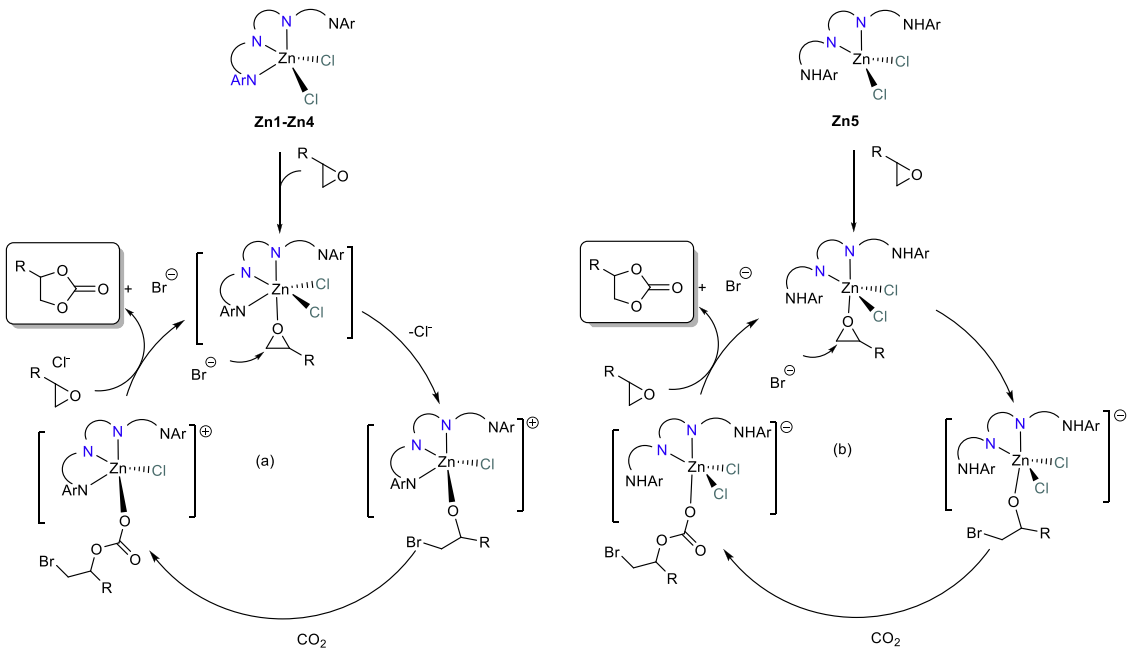

Scheme 5. Proposed CO_2/epoxide cycloaddition mechanisms for (a) Zn1-Zn4/TBAB and (b) Zn5/TBAB catalytic systems.

observed higher activity of **Zn1** in comparison to **Zn2** and **Zn3**, and the also higher activity of **Zn5,** which stabilises species with lower coordination number, *versus* **Zn4**.

It is also possible for a chloride ligand of **Zn1** to dissociate (Scheme 5a). In this case the substitution of the carbonate by the free chloride would also favour the release of the product and the recovery of the catalyst, given that in the case of complexes **Zn1** to **Zn4** tetracoordinate species are significantly less stable than pentacoordinate ones, especially in the case of the more hindered **Zn1** with large isopropyl substituents.

In the case of the tetrahedral **Zn5** complex, the pentacoordinate species may form by coordination of the epoxide without dissociation of the chloride ligand (Scheme 5b) given that the ΔG between five- and four-coordinate species are small (ΔG *ca* 4 kcal/mol).

Furthermore, the rigid zinc-phenanthroline skeleton (**Zn1-Zn3**) may control the equilibrium towards the formation of some specific isomers, favoring thus the reactivity of the intermediates. In contrast, the more flexible bipyridine systems **Zn4** and **Zn5** may produce different isomers and even bimetallic species as reported previously with related compounds [63] giving place to less active systems. But in the case of the amine bipyridine derivative **Zn5**, an interaction of the free amine with CO_2 cannot be ruled out too, what will explain its higher activity than that of the **Zn4**/TBAB system.

A computational study on the reaction mechanism is in progress to determine the possible reaction paths locating the reaction intermediates and transition states to calculate the energy barriers of the different steps of the reaction and elucidate the reaction mechanism. This information should explain the observed trends of the activity of the series of complexes experimentally studied to allow predicting further modifications of the catalytic system to improve their efficiency.

4. Conclusions

Zn(II) complexes with easy-to-modify N4-donor ligands derived from phenanthroline- and bipyridine-bis(aniline) have been synthetized and characterized by spectroscopic methods, X-ray diffraction in solid state and a computational study. They show high selectivity as catalysts for the synthesis of cyclic carbonates obtained from addition of CO_2 to terminal epoxides, the catalytic system is stable under catalytic conditions and can be used in a semi-batch process for several cycles adding fresh epoxide and CO_2, but the activity leaves room for improvement. The systematic study of the structural parameters and the nature of the functional groups allowed identifying the best catalyst (those with the phenanthroline skeleton and with bulky substituents in the *orto*-aniline position). Additionally, the computational calculations about the relative stability of the different conformers of the catalysts corroborate the experimental observations, that the complexes with coordination numbers 4 and 5 are more stable than those hexacoordinated and that the imine complexes prefer to form 5-coordinated species while the bipyridine bis(amine) **Zn5** stabilises preferentially the 4-coordinated complex.

The results of this combined experimental-computational work provide an essential information to be able to design better catalytic systems, although further knowledge about the mechanism of the reaction is also necessary. This study, out of the scope of this paper, will be developed soon.

Supplementary data

Supplementary data associated with this article can be found, in the online version. Deposition numers CCDC-2173739, CCDC-2173741 and CCDC-2173740 contain the supplementary crystallographic data for this paper corresponding to **Zn1, Zn2** and **Zn5** complexes respectively.

CRediT authorship contribution statement

Nassima El Aouni: Investigation. **Claudia López Redondo:** Investigation. **Md Bin Yeamin:** Investigation. **Ali Aghmiz:** Supervision, Funding acquisition. **Mar Reguero:** Conceptualization, Supervision, Investigation, Writing – review & editing, Funding acquisition. **Anna M. Masdeu-Bultó:** Conceptualization, Writing – review & editing, Supervision, Funding acquisition, Investigation.

Declaration of Competing Interest

The authors declare the following financial interests/personal relationships which may be considered as potential competing interests: Anna M. Masdeu-Bulto reports financial support was provided by Spain Ministry of Science and Innovation. Anna M. Masdeu-Bulto reports financial support was provided by Generalitat of Catalonia Department of Research And Universities. Ali Aghmiz reports financial support was

provided by Government of the Kingdom of Morocco. Mar Reguero reports financial support was provided by Spain Ministry of Science and Innovation. Mar reguero reports was provided by Generalitat of Catalonia Department of Research And Universities.

Data availability

Data will be made available on request.

Acknowledgements

The authors are thankful to the Spanish Ministerio de Ciencia e Innovación and AEI/FEDER UE (PID2019-104427RB-100 and PID2020-113187GB-I00), the Generalitat de Catalunya Departament de Recerca i Universitats (2021 SGR 00163, 2021 SGR 00110 and N. El Aouni grant 2019_FIB 00784) and Xarxa d'R+D+I en Química Computacional (XRQTC) and The Centre National pour la Recherche Scientifique et Technique (CNRST / Maroc) (Programme PBER N°: 9UAE2019).

Supplementary materials

Supplementary material associated with this article can be found, in the online version, at doi:10.1016/j.mcat.2023.112992.

References

[1] B. Schäffner, F. Schäffner, S.P. Verevkin, A. Börner, Organic carbonates as solvents in synthesis and catalysis, Chem. Rev. 110 (2010) 4554–4581, https://doi.org/10.1021/cr900393d.
[2] J.S. Bello Forero, J.A. Hernández Muñoz, J. Jones Junior, F.M. da Silva, Propylene carbonate in organic synthesis: exploring its potential as a green solvent, Curr. Org. Synth. 13 (2016) 834–846, https://doi.org/10.2174/1570179413999160211094705.
[3] C.M. Alder, J.D. Hayler, R.K. Henderson, A.M. Redman, L. Shukla, L.E. Shuster, H. F. Sneddon, Updating and further expanding GSK's solvent sustainability guide, Green Chem. 18 (2016) 3879–3890, https://doi.org/10.1039/c6gc00611f.
[4] H. Zhao, S.J. Park, F. Shi, Y. Fu, V. Battaglia, P.N. Ross, G. Liu, Propylene carbonate (PC)-based electrolytes with high coulombic efficiency for lithium-ion batteries, J. Electrochem. Soc. 161 (2014) 194–200, https://doi.org/10.1149/2.095401jes.
[5] A.A.G. Shaikh, S. Sivaram, Organic carbonates, Chem. Rev. 96 (1996) 951–976, https://doi.org/10.1021/cr950067i.
[6] S. Gennen, B. Grignard, T. Tassaing, C. Jérôme, C. Detrembleur, CO_2 -sourced α-alkylidene cyclic carbonates: a step forward in the quest for functional regioregular poly(urethane)s and poly(carbonate)s, Angew. Chem. Int. Ed. 56 (2017) 10394–10398, https://doi.org/10.1002/anie.201704467.
[7] L. Ruiz, A. Aghmiz, A.M. Masdeu-Bultó, G. Lligadas, J.C. Ronda, M. Galià, V. Cádiz, Upgrading castor oil: from heptanal to non-isocyanate poly(amide-hydroxyurethane)s, Polymer 124 (2017) 226–234, https://doi.org/10.1016/j.polymer.2017.07.070 (Guildf).
[8] G.L. Gregory, E.M. Lopez-Vidal, A. Buchard, Polymers from sugars: cyclic monomer synthesis, ring-opening polymerisation, material properties and applications, Chem. Commun. 53 (2017) 2198–2217, https://doi.org/10.1039/c6cc09578j.
[9] W. Guo, J.E. Gómez, À. Cristòfol, J. Xie, A.W. Kleij, Catalytic transformations of functionalized cyclic organic carbonates, Angew. Chem. Int. Ed. 57 (2018) 13735–13747, https://doi.org/10.1002/anie.201805009.
[10] J.H. Clements, Reactive applications of cyclic alkylene carbonates, Ind. Eng. Chem. Res. 42 (2003) 663–674, https://doi.org/10.1021/ie020678i.
[11] H.J. Buysch, Carbonic Esters. Ullmann's Encyclopedia of Industrial Chemistry, Wiley-VCH Verlag GmbH & Co. KGaA, Weinheim, Germany, 2000, pp. 45–71, https://doi.org/10.1002/14356007.a05_197.
[12] M. Alves, B. Grignard, R. Mereau, C. Jerome, T. Tassaing, C. Detrembleur, Organocatalyzed coupling of carbon dioxide with epoxides for the synthesis of cyclic carbonates: catalyst design and mechanistic studies, Catal. Sci. Technol. 7 (2017) 2651–2684, https://doi.org/10.1039/C7CY00438A.
[13] V. Caló, A. Nacci, A. Monopoli, A. Fanizzi, Cyclic carbonate formation from carbon dioxide and oxiranes in tetrabutylammonium halides as solvents and catalysts, Org. Lett. 4 (2002) 2561–2563, https://doi.org/10.1021/ol026189w.
[14] M. Cokoja, M.E. Wilhelm, M.H. Anthofer, W.A. Herrmann, F.E. Kühn, Synthesis of cyclic carbonates from epoxides and carbon dioxide by using organocatalysts, ChemSusChem 8 (2015) 2436–2454, https://doi.org/10.1002/cssc.201500161.
[15] R. Hua, S. Roy, Organocatalytic transformation of carbon dioxide. Recent Advances in Organocatalysis, InTech, 2016, pp. 87–106, https://doi.org/10.5772/63096.
[16] G. Fiorani, W. Guo, A.W. Kleij, Sustainable conversion of carbon dioxide: the advent of organocatalysis, Green Chem. 17 (2015) 1375–1389, https://doi.org/10.1039/c4gc01959h.
[17] J. Sun, S. Fujita, M. Arai, Development in the green synthesis of cyclic carbonate from carbon dioxide using ionic liquids, J. Organomet. Chem. 690 (2005) 3490–3497, https://doi.org/10.1016/j.jorganchem.2005.02.011.
[18] Q. He, J.W. O'Brien, K.A. Kitselman, L.E. Tompkins, G.C.T. Curtis, F.M. Kerton, Synthesis of cyclic carbonates from CO_2 and epoxides using ionic liquids and related catalysts including choline chloride-metal halide mixtures, Catal. Sci. Technol. 4 (2014) 1513–1528, https://doi.org/10.1039/c3cy00998j.
[19] B.H. Xu, J.Q. Wang, J. Sun, Y. Huang, J.P. Zhang, X.P. Zhang, S.J. Zhang, Fixation of CO_2 into cyclic carbonates catalyzed by ionic liquids: a multi-scale approach, Green Chem. 17 (2015) 108–122, https://doi.org/10.1039/C4GC01754D.
[20] Y. Chen, T. Mu, Conversion of CO_2 to value-added products mediated by ionic liquids, Green Chem. 21 (2019) 2544–2574, https://doi.org/10.1039/C9GC00827F.
[21] S. Sopeña, G. Fiorani, C. Martín, A.W. Kleij, Highly efficient organocatalyzed conversion of oxiranes and CO_2 into organic carbonates, ChemSusChem 8 (2015) 3248–3254, https://doi.org/10.1002/cssc.201500710.
[22] K.R. Roshan, A.C. Kathalikkattil, J. Tharun, D.W. Kim, Y.S. Won, D.W. Park, Amino acid/KI as multi-functional synergistic catalysts for cyclic carbonate synthesis from CO_2 under mild reaction conditions: a DFT corroborated study, Dalton Trans. 43 (2014) 2023–2031, https://doi.org/10.1039/c3dt52830h.
[23] L. Martínez-Rodríguez, J. OtaloraGarmilla, A.W. Kleij, Cavitand-based polyphenols as highly reactive organocatalysts for the coupling of carbon dioxide and oxiranes, ChemSusChem 9 (2016) 749–755, https://doi.org/10.1002/cssc.201501463.
[24] S. Arayachukiat, C. Kongtes, A. Barthel, S.V.C. Vummaleti, A. Poater, S. Wannakao, L. Cavallo, V. D'Elia, Ascorbic acid as a bifunctional hydrogen bond donor for the synthesis of cyclic carbonates from CO_2 under ambient conditions, ACS Sustain. Chem. Eng. 5 (2017) 6392–6397, https://doi.org/10.1021/acssuschemeng.7b01650.
[25] N. Liu, Y.F. Xie, C. Wang, S.J. Li, D. Wei, M. Li, B. Dai, Cooperative multifunctional organocatalysts for ambient conversion of carbon dioxide into cyclic carbonates, ACS Catal. 8 (2018) 9945–9957, https://doi.org/10.1021/acscatal.8b01925.
[26] K. Kossev, N. Koseva, K. Troev, Calcium chloride as co-catalyst of onium halides in the cycloaddition of carbon dioxide to oxiranes, J. Mol. Catal. A Chem. 194 (2003) 29–37, https://doi.org/10.1016/S1381-1169(02)00513-7.
[27] M.E. Wilhelm, M.H. Anthofer, R.M. Reich, V. D'Elia, J.M. Basset, W.A. Herrmann, M. Cokoja, F.E. Kühn, Niobium(v) chloride and imidazolium bromides as efficient dual catalyst systems for the cycloaddition of carbon dioxide and propylene oxide, Catal. Sci. Technol. 4 (2014) 1638–1643, https://doi.org/10.1039/c3cy01057k.
[28] K. Yamaguchi, K. Ebitani, T. Yoshida, H. Yoshida, K. Kaneda, Mg-Al mixed oxides as highly active acid-base catalysts for cycloaddition of carbon dioxide to epoxides, J. Am. Chem. Soc. 121 (1999) 4526–4527, https://doi.org/10.1021/ja9902165.
[29] J.W. Comerford, I.D.V. Ingram, M. North, X. Wu, Sustainable metal-based catalysts for the synthesis of cyclic carbonates containing five-membered rings, Green Chem. 17 (2015) 1966–1987, https://doi.org/10.1039/c4gc01719f.
[30] A. Decortes, A.M. Castilla, A.W. Kleij, Salen-complex-mediated formation of cyclic carbonates by cycloaddition of CO_2 to epoxides, Angew. Chem. Int. Ed. 49 (2010) 9822–9837, https://doi.org/10.1002/anie.201002087.
[31] J. Meléndez, M. North, R. Pasquale, Synthesis of cyclic carbonates from atmospheric pressure carbon dioxide using exceptionally active aluminium(salen) complexes as catalysts, Eur. J. Inorg. Chem. (2007) 3323–3326, https://doi.org/10.1002/ejic.200700521.
[32] L. Cuesta-Aluja, A. Campos-Carrasco, J. Castilla, M. Reguero, A.M. Masdeu-Bultó, A. Aghmiz, Highly active and selective Zn(II)-NN′O Schiff base catalysts for the cycloaddition of CO_2 to epoxides, J. CO2 Util. 14 (2016) 10–22, https://doi.org/10.1016/j.jcou.2016.01.002.
[33] C. Maeda, T. Taniguchi, K. Ogawa, T. Ema, Bifunctional catalysts based on m-phenylene-bridged porphyrin dimer and trimer platforms: synthesis of cyclic carbonates from carbon dioxide and epoxides, Angew. Chem. Int. Ed. 54 (2015) 134–138, https://doi.org/10.1002/anie.201409729.
[34] T. Ema, Y. Miyazaki, J. Shimonishi, C. Maeda, J.Y. Hasegawa, Bifunctional porphyrin catalysts for the synthesis of cyclic carbonates from epoxides and CO_2 : structural optimization and mechanistic study, J. Am. Chem. Soc. 136 (2014) 15270–15279, https://doi.org/10.1021/ja507665a.
[35] P.T.K. Nguyen, H.T.D. Nguyen, H.N. Nguyen, C.A. Trickett, Q.T. Ton, E. Gutiérrez-Puebla, M.A. Monge, K.E. Cordova, F. Gándara, New metal-organic frameworks for chemical fixation of CO_2, ACS Appl. Mater. Interfaces 10 (2018) 733–744, https://doi.org/10.1021/acsami.7b16163.
[36] M.H. Beyzavi, C.J. Stephenson, Y. Liu, O. Karagiaridi, J.T. Hupp, O.K. Farha, Metal-organic framework-based catalysts: chemical fixation of CO_2 with epoxides leading to cyclic organic carbonates, Front. Energy Res. 2 (2015) 1–10, https://doi.org/10.3389/fenrg.2014.00063.
[37] T. Sakakura, J.C. Choi, H. Yasuda, Transformation of carbon dioxide, Chem. Rev. 107 (2007) 2365–2387, https://doi.org/10.1021/cr068357u.
[38] G.W. Coates, D.R. Moore, Discrete metal-based catalysts for the copolymerization of CO_2 and epoxides: discovery, reactivity, optimization, and mechanism, Angew. Chem. Int. Ed. 43 (2004) 6618–6639, https://doi.org/10.1002/anie.200460442.
[39] C. Martín, G. Fiorani, A.W. Kleij, Recent advances in the catalytic preparation of cyclic organic carbonates, ACS Catal. 5 (2015) 1353–1370, https://doi.org/10.1021/cs5018997.
[40] P.P. Pescarmona, M. Taherimehr, Challenges in the catalytic synthesis of cyclic and polymeric carbonates from epoxides and CO_2, Catal. Sci. Technol. 2 (2012) 2169–2187, https://doi.org/10.1039/c2cy20365k.
[41] M. North, R. Pasquale, C. Young, Synthesis of cyclic carbonates from epoxides and CO_2, Green Chem. 12 (2010) 1514–1539, https://doi.org/10.1039/c0gc00065e.

[42] R.R. Shaikh, S. Pornpraprom, V. D'Elia, Catalytic strategies for the cycloaddition of pure, diluted, and waste CO_2 to epoxides under ambient conditions, ACS Catal. 8 (2018) 419–450, https://doi.org/10.1021/acscatal.7b03580.

[43] R. Dalpozzo, N. Della Ca', B. Gabriele, R. Mancuso, Recent advances in the chemical fixation of carbon dioxide: a green route to carbonylated heterocycle synthesis, Catalysts 9 (2019) 511, https://doi.org/10.3390/catal9060511.

[44] N.J. English, M.M. El-Hendawy, D.A. Mooney, J.M.D. MacElroy, Perspectives on atmospheric CO_2 fixation in inorganic and biomimetic structures, Coord. Chem. Rev. 269 (2014) 85–95, https://doi.org/10.1016/j.ccr.2014.02.015.

[45] D.J. Darensbourg, S.A. Niezgoda, J.D. Draper, J.H. Reibenspies, Mechanistic aspects of the copolymerization of CO_2 and epoxides by soluble zinc bis (phenoxide) catalysts as revealed by their cadmium analogues, J. Am. Chem. Soc. 120 (1998) 4690–4698, https://doi.org/10.1021/ja9801487.

[46] I. Karamé, S. Zaher, N. Eid, L. Christ, New zinc/tetradentate N4 ligand complexes: efficient catalysts for solvent-free preparation of cyclic carbonates by CO_2/epoxide coupling, Mol. Catal. 456 (2018) 87–95, https://doi.org/10.1016/J.MCAT.2018.07.001.

[47] M. Adolph, T.A. Zevaco, O. Walter, E. Dinjus, M. Döring, Easy-to-handle ionic transition metal complexes in the formation of carbonates from epoxides and CO_2: a N 4-ligand system based on N,N-bis(2-pyridinecarboxamide)-1,2-benzene, Polyhedron 48 (2012) 92–98, https://doi.org/10.1016/j.poly.2012.09.011.

[48] M. Adolph, T. a Zevaco, C. Altesleben, O. Walter, E. Dinjus, New cobalt, iron and chromium catalysts based on easy-to-handle N4-chelating ligands for the coupling reaction of epoxides with CO_2, Dalton Trans. 43 (2014) 3285–3296, https://doi.org/10.1039/c3dt53084a.

[49] M. Adolph, T.A. Zevaco, C. Altesleben, S. Staudt, E. Dinjus, New zinc catalysts based on easy-to-handle N<inf>4</inf>-chelating ligands for the coupling reaction of epoxides with CO_2, J. Mol. Catal. A Chem. 400 (2015) 104–110, https://doi.org/10.1016/j.molcata.2015.01.028.

[50] M.A. Fuchs, S. Staudt, C. Altesleben, O. Walter, T.A. Zevaco, E. Dinjus, A new air-stable zinc complex based on a 1,2-phenylene-diimino-2- cyanoacrylate ligand as an efficient catalyst of the epoxide-CO_2 coupling, Dalton Trans. 43 (2014) 2344–2347, https://doi.org/10.1039/c3dt52927d.

[51] E. Mercadé, E. Zangrando, C. Claver, C. Godard, Robust zinc complexes that contain pyrrolidine-based ligands as recyclable catalysts for the synthesis of cyclic carbonates from carbon dioxide and epoxides, ChemCatChem 8 (2016) 234–243, https://doi.org/10.1002/cctc.201500772.

[52] A. Angeloff, J.C. Daran, J. Bernadou, B. Meunier, The ligand 1,10-phenanthroline-2,9-dicarbaldehyde dioxime can act both as a tridentate and as a tetradentate ligand – synthesis, characterization and crystal structures of its transition metal complexes, Eur. J. Inorg. Chem. 2000 (2000) 1985–1996, https://doi.org/10.1002/1099-0682(200009)2000:9<1985::AID–EJIC1985>3.0.CO;2-K.

[53] L.F. Hernández-Ayala, M. Flores-Álamo, S. Escalante-Tovar, R. Galindo-Murillo, J. C. García-Ramos, J. García-Valdés, V. Gómez-Vidales, K. Reséndiz-Acevedo, Y. Toledano-Magaña, L. Ruiz-Azuara, Synthesis, characterization, theoretical studies and biological activity of coordination compounds with essential metals containing N4-donor ligand 2,9-di(ethylaminomethyl)-1,10-phenanthroline, Inorg. Chim. Acta 470 (2018) 187–196, https://doi.org/10.1016/j.ica.2017.06.040.

[54] Y.D.M. Champouret, J.D. Maréchal, R.K. Chaggar, J. Fawcett, K. Singh, F. Maseras, G.A. Solan, Factors affecting imine coordination in (iminoterpyridine)MX2 (M = Fe, Co, Ni, Zn): synthesis, structures, DFT calculations and ethylene oligomerisation studies, New J. Chem. 31 (2007) 75–85, https://doi.org/10.1039/b610562a.

[55] K. Naveen, H. Ji, T.S. Kim, D. Kim, D.H. Cho, C3-symmetric zinc complexes as sustainable catalysts for transforming carbon dioxide into mono- and multi-cyclic carbonates, Appl. Catal. B Environ. 280 (2021), 119395, https://doi.org/10.1016/j.apcatb.2020.119395.

[56] M. Cavalleri, N. Panza, A. di Biase, G. Tseberlidis, S. Rizzato, G. Abbiati, A. Caselli, [Zinc(II)(Pyridine-Containing Ligand)] complexes as single-component efficient catalyst for chemical fixation of CO_2 with epoxides, Eur. J. Org. Chem. 2021 (2021) 2764–2771, https://doi.org/10.1002/ejoc.202100409.

[57] M. Alonso De La Peña, L. Merzoud, W. Lamine, A. Tuel, H. Chermette, L. Christ, Robust pyrrole-Schiff base Zinc complexes as novel catalysts for the selective cycloaddition of CO_2 to epoxides, J. CO2 Util. 44 (2021) 1–16, https://doi.org/10.1016/j.jcou.2020.101380.

[58] F.W. Lewis, L.M. Harwood, M.J. Hudson, M.G.B. Drew, J.F. Desreux, G. Vidick, N. Bouslimani, G. Modolo, A. Wilden, M. Sypula, T.H. Vu, J.P. Simonin, Highly efficient separation of actinides from lanthanides by a phenanthroline-derived bis-triazine ligand, J. Am. Chem. Soc. 133 (2011) 13093–13102, https://doi.org/10.1021/ja203378m.

[59] X.B. Lu, H. Wang, R. He, Aluminum phthalocyanine complex covalently bonded to MCM-41 silica as heterogeneous catalyst for the synthesis of cyclic carbonates, J. Mol. Catal. A Chem. 186 (2002) 33–42, https://doi.org/10.1016/S1381-1169(02)00181-4.

[60] P.D. Beer, J. Danks, M.G.B. Drew, J.F. McAleer, Redox-active lithium-selective ionophores based on new 2,9-bis(ferrocenyl) substituted phenanthroline derivatives, J. Organomet. Chem. 476 (1994) 63–72, https://doi.org/10.1016/0022-328X(94)84141-1.

[61] G.R. Newkome, H.W. Lee, 18[Hexa(2,6)P*yridinoécoronand*-6]: "Sexipyridine", J. Am. Chem. Soc. 105 (1983) 5956–5957, https://doi.org/10.1021/ja00356a061.

[62] Z. Yang, J.M. Lehn, Dynamic covalent self-sorting and kinetic switching processes in two cyclic orders: macrocycles and macrobicyclic cages, J. Am. Chem. Soc. 142 (2020) 15137–15145, https://doi.org/10.1021/jacs.0c07131.

[63] G.A. Griffith, M.J. Al-Khatib, K. Patel, K. Singh, G.A. Solan, Solid and solution state flexibility of sterically congested bis(imino)bipyridine complexes of zinc(II) and nickel(II), Dalton Trans. 2 (2009) 185–196, https://doi.org/10.1039/B811309B.

[64] R.H. Blessing, An empirical correction for absorption anisotropy, Acta Crystallogr. Sect. A 51 (1995) 33–38, https://doi.org/10.1107/S0108767394005726.

[65] M.C. Burla, R. Caliandro, B. Carrozzini, G.L. Cascarano, C. Cuocci, C. Giacovazzo, M. Mallamo, A. Mazzone, G. Polidori, Crystal structure determination and refinement via SIR2014, J. Appl. Crystallogr. 48 (2015) 306–309, https://doi.org/10.1107/S1600576715001132.

[66] G.M. Sheldrick, Crystal structure refinement with SHELXL, Acta Crystallogr. Sect. C Struct. Chem. 71 (2015) 3–8, https://doi.org/10.1107/S2053229614024218.

[67] C.B. Hübschle, G.M. Sheldrick, B. Dittrich, ShelXle: a Qt graphical user interface for SHELXL, J. Appl. Crystallogr. 44 (2011) 1281–1284, https://doi.org/10.1107/S0021889811043202.

[68] A. Technologies, ABSPACK SCALE3. Empirical absorption Correction.CrysAlisPro. Rigaku Oxford Difracction. Agilent Tecnologies, 2018, Version 1.171.40.35a.

[69] D.R. Lide (Ed.), CRC Handbook of Chemistry and Physics, 81st ed., CRC Press, Boca Raton, 2000.

[70] S. Grimme, Supramolecular binding thermodynamics by dispersion-corrected density functional theory, Chem. Eur. J. 18 (2012) 9955–9964, https://doi.org/10.1002/chem.201200497.

[71] G.J.P. Britovsek, S.P.D. Baugh, O. Hoarau, V.C. Gibson, D.F. Wass, A.J.P. White, D. J. Williams, The role of bulky substituents in the polymerization of ethylene using late transition metal catalysts: a comparative study of nickel and iron catalyst systems, Inorg. Chim. Acta 345 (2003) 279–291, https://doi.org/10.1016/S0020-1693(02)01293-8.

[72] S. Zai, H. Gao, Z. Huang, H. Hu, H. Wu, Q. Wu, Substituent effects of pyridine-amine nickel catalyst precursors on ethylene polymerization, ACS Catal. 2 (2012) 433–440, https://doi.org/10.1021/cs200593c.

[73] H.H. Perkampus, W. Rother, Die infrarot- und ramanspektren der phenanthroline, Spectrochim. Acta Part A Mol. Spectrosc. 30 (1974) 597–610, https://doi.org/10.1016/0584-8539(74)80183-2.

[74] A.W. Addison, T.N. Rao, J. Reedijk, J. van Rijn, G.C. Verschoor, Synthesis, structure, and spectroscopic properties of copper(II) compounds containing nitrogen–sulphur donor ligands; the crystal and molecular structure of aqua[1,7-*bis*(N-*methylbenzimidazol-2′-yl*)-2,6-*dithiaheptane*]copper(II) perchlorate, J. Chem. Soc. Dalton Trans. 251 (1984) 1349–1356, https://doi.org/10.1039/DT9840001349.

[75] L. Wang, W.H. Sun, L. Han, H. Yang, Y. Hu, X. Jin, Late transition metal complexes bearing 2,9-bis(imino)-1,10-phenanthrolinyl ligands: synthesis, characterization and their ethylene activity, J. Organomet. Chem. 658 (2002) 62–70, https://doi.org/10.1016/S0022-328X(02)01623-6.

[76] A. Begum, O. Seewald, U. Flörke, G. Henkel, Structural and NMR spectroscopic investigations of CuI, CuII, NiII, ZnII and FeII complexes of 2, 9-di-(benzothiazolino)-1,10-phenanthroline, ChemistrySelect 1 (2016) 2257–2264, https://doi.org/10.1002/slct.201600505.

[77] S. Ameerunisha, J. Schneider, T. Meyer, P.S. Zacharias, E. Bill, G. Henkel, Synthesis and structural characterisation of Fe(II) and Cu(I) complexes of a new tetrafunctional N-donor ligand with dodecahedral or tetrahedral binding domains, Chem. Commun. (2000) 2155–2156, https://doi.org/10.1039/b005671p.

[78] R.D. Shannon, Revised effective ionic radii and systematic studies of interatomic distances in halides and chalcogenides, Acta Crystallogr. Sect. A 32 (1976) 751–767, https://doi.org/10.1107/S0567739476001551.

[79] J. Tharun, K.R. Roshan, A.C. Kathalikkattil, D.H. Kang, H.M. Ryu, D.W. Park, Natural amino acids/H_2O as a metal- and halide-free catalyst system for the synthesis of propylene carbonate from propylene oxide and CO_2 under moderate conditions, RSC Adv. 40 (2014) 41266–41270, https://doi.org/10.1039/c4ra06964a.

[80] H. Kisch, R. Millini, I.J. Wang, Bifunktionelle katalysatoren zur synthese cyclischer carbonate aus oxiranen und kohlendioxid, Chem. Ber. 119 (1986) 1090–1094, https://doi.org/10.1002/cber.19861190329.

[81] J. Sun, S.I. Fujita, F. Zhao, M. Arai, A highly efficient catalyst system of ZnBr2/n-Bu4NI for the synthesis of styrene carbonate from styrene oxide and supercritical carbon dioxide, Appl. Catal. A Gen. 287 (2005) 221–226, https://doi.org/10.1016/j.apcata.2005.03.035.

[82] H. Vignesh Babu, K. Muralidharan, Zn(ii), Cd(ii) and Cu(ii) complexes of 2,5-bis(N-(2,6-diisopropylphenyl)iminomethyl)pyrrole: synthesis, structures and their high catalytic activity for efficient cyclic carbonate synthesis, J. Chem. Soc. Dalton Trans. 42 (2013) 1238–1248, https://doi.org/10.1039/c2dt31755a.